Tetrahedron xxx (xxxx) xxx

Contents lists available at ScienceDirect

Tetrahedron

journal homepage: www.elsevier.com/locate/tet

# Convenient synthesis of regioisomerically pure 5- and 6-functionalized xanthene dyes via $S_NAr$ reaction and comparison of their reactivity towards click reaction

Masaya Mori, Yuuta Fujikawa*, Hideshi Inoue

*School of Life Sciences, Tokyo University of Pharmacy and Life Sciences, 1432-1 Horinouchi, Hachioji, Tokyo, 192-0392, Japan*

ARTICLE INFO

*Article history:*
Received 3 December 2019
Received in revised form
24 February 2020
Accepted 26 February 2020
Available online xxx

*Keywords:*
Fluorescent dye
Chemical equilibrium
$S_NAr$ reaction
SPAAC

ABSTRACT

In this study, we present an efficient and general strategy for the individual preparation of both isomers of 5(6)-functionalized xanthene-based fluorophores. Spectroscopic analysis of the acid-base equilibrium of 5(6)-nitro xanthene dyes has shown that they exist predominantly in the colorless spirolactone form in certain aprotic dipolar solvents. In such solvents, regioisomerically selective *ipso*-substitution of the nitro group by sodium azide occurs at the 6- position but not at the 5- position due to the electron-withdrawing spirolactone moiety at the *para*-position, relative to the nitro group. This reaction allows the separation of the isomer with the 6-azide group and the intact 5-nitro isomer. The 5-nitro group of the latter was then reduced to an amino group and subsequently converted to an azide group. This strategy enables the preparation of both the 5- and 6-functionalized isomers individually from a mixture of precursors, which is otherwise unachievable. The azide isomers were then compared in reactivity by strain-promoted azide-alkyne cycloaddition (SPAAC) with bicycle[6.1.0]non-4-yene (BCN).



## 1. Introduction

Xanthene-based dyes, such as fluoresceins and rhodamines, are widely used in various bioassays as labeling agents and fluorescence probes, because they have a variety of visible light emissions ranging from blue-green to red, a high molar extinction coefficient and quantum efficacy, high water-solubility, and are easy to synthesize and derivatize [1,2].

Since xanthene dyes are composed of a *meso*-phenyl ring and a xanthene moiety, they can be derivatized to give various functions by modifying the phenyl-ring moiety while retaining water-solubility and resistance to self-aggregation. In this context, 5- or 6-functionalization of the *meso*-phenyl ring in the xanthene derivatives is crucial for the synthesis of fluorogenic probes and for the modification and bioconjugation of biopolymers [3]. For example, 5(6)-aminofluorescein is a key intermediate to lead to the respective isothiocyanate (ITC), iodo (-I), and azide (-$N_3$) derivatives [4]. These 5(6)-functionalized fluorescein derivatives have been used as labeling agents of target proteins [5,6], synthetic intermediates for coupling reactions [7,8], fluorogenic probes [9,10], and have also been applied to the click reaction [11,12].

However, previously reported biological applications of different regioisomers have shown different results between the isomers [13,14]. In addition, fluorogenic probes based on 5- and 6-functionalized fluorescein derivatives were reported to show differences in target selectivity [15] or enzymatic kinetic parameters [16] between regioisomers. These examples suggest that sensing applications should be performed with both isomers to avoid misinterpretation based on the results obtained with only one isomer. Further, to developing more sophisticated probes, it is desirable to assess the sensing performance (e.g. selectivity and reactivity) of fluorogenic probes for each regioisomer.

A typical synthetic procedure based on the acid catalyzed condensation of asymmetric 4-functionalized phthalic anhydride and resorcinol or aminophenol produces a regioisomeric mixture of 5(6)-functionalized xanthene-based dyes. To address this problem, numerous efforts have been dedicated to separate the isomers of xanthene derivatives by fractional recrystallization [4,17,18] or to prepare a single isomer with the use of an asymmetric starting material [19]. These approaches have often been applied to the preparation of pure regioisomers of 5- and 6-carboxyfluorescein. In contrast, synthetic procedures for the preparation of pure isomers functionalized with an azide or amino group at the 5- or 6-position

* Corresponding author.
*E-mail address:* yfuji@toyaku.ac.jp (Y. Fujikawa).

https://doi.org/10.1016/j.tet.2020.131087
0040-4020/

have not been reported. This is partly because xanthene dyes with a nitro group at the 5- or 6-position have similar physicochemical properties to each other, which prevents fractional recrystallization. Malakhov and Burgess succeeded in the synthesis of pure regioisomeric 5-functionalized 2′, 7′-dichlorofluorescein (DCF) by recrystallization [20]. Although the 5-isomer is useful by itself, the 6-isomer is not obtained by this approach, so that it is impossible to compare the labeling kinetics and optical properties of the two isomers.

Here we present a simple synthetic strategy based on the regioisomer selective $S_NAr$ azidation that selectively provides individual azide- or amino-functionalized regioisomers. Optimization of the aprotic dipolar solvent used shifts the equilibrium between the open and closed form completely to a closed spirolactone, allowing the *ipso*-substitution of the nitro group at 6-position. Based on this, both regioisomers were prepared for two fluorophores, DCF and tetramethylrhodamine (TMR), allowing for comparison of their reactivity and changes in their spectroscopic properties. Then 5-$N_3$DCF was compared with the 6-isomer in reactivity by strain-promoted azide-alkyne cycloaddition (SPAAC) with bicycle[6.1.0]non-4-yene (BCN). Our new synthetic method allows for the convenient regioselective preparation of functionalized xanthene dyes and facilitates the development of new labeling dyes that can be used in the field of biochemistry and chemical biology.

## 2. Materials and methods

### 2.1. General procedures

All reagents were purchased from commercial suppliers and used without further purification. $^1$H and $^{13}$C NMR spectra were obtained with the DRX-400 spectrometer (Bruker, Billerica, MA, USA) at 400 and 100 MHz, respectively. Chemical shifts (δ) were calibrated to the solvent peak (δ 2.49 and 39.5 for $^1$H and $^{13}$C NMR in DMSO-$d_6$). A precoated thin layer chromatography (TLC) plate (Merck, silica gel 60 $F_{254}$, No. 1.05715.0001) was used for TLC analysis. Column chromatography was performed with silica gel (200−300 mesh) (Kanto Chem. Inc.). High resolution mass spectra (HRMS) were obtained from a micro mass LCT spectrometer (Waters, Milford, MA, USA) under positive or negative electro spray ionization ($ESI^+$ or $ESI^-$) conditions. The absorption spectra of each compound (50 μM) were measured with a V-550 UV/VIS spectrophotometer (JASCO Corp., Tokyo, Japan).

### 2.2. HPLC analysis

HPLC analysis was performed on a HPLC system composed of a pump (LC-20AT, Shimadzu) and a photodiode array detector (SPD-M20A, Shimadzu). Clarity software (DataApex, Czech Republic) was used for operation of the system and data analysis. For the time course analysis, 1.5 μL of the reaction mixture was taken and mixed with in 1.5 ml of 10 mM ammonium acetate containing 200 μM DCF. The solution (25 μL) was injected and subjected to the analysis. Separation was achieved on a Mightysil RP-18 GP column (250 mm × 4.6 mm (5 μm); Kanto Chemical, Tokyo, Japan) Eluent A: B = 85: 15 → 50: 50 (20 min) → 50: 50 (30 min) at a flow rate of 1.0 ml/min. A: 10 mM ammonium acetate, B: MeCN.

### 2.3. Organic synthesis

#### 2.3.1. 5(6)-Nitro-2′,7′-dichlorofluorescein (5(6)-$NO_2$DCF)

A suspension of 4-nitrophthalic anhydride (2.05 g, 10.6 mmol) and 4-chlororesorcinol (4.63 g, 32.0 mmol) in $CH_3SO_3H$ (5 ml) was stirred at 100 °C for 11 h. After the mixture cooled to room temperature, it was poured onto $H_2O$ (100 ml) on ice. The mixture was basified with 10 N NaOH to pH 14 and stirred at room temperature. The mixture was acidified with concentrated HCl to pH 2 and the precipitate was collected by filtration and washed three times with ice-cold $H_2O$. The residue was purified by silica gel column chromatography ($CHCl_3$/MeOH = 10/1 to 2/1) to yield **5(6)-$NO_2$DCF** as an orange solid (2.75 g, 6.16 mmol, yield 58%).

#### 2.3.2. 6-Azido-2′,7′ -dichlorofluorescein (6-$N_3$DCF), 5-nitro-2′,7′-dichlorofluorescein (6-$NO_2$DCF)

To a suspension of **5(6)-$NO_2$DCF** (467 mg, 1.05 mmol, 5-isomer: 6-isomer = 1:1) in HMPA (2 ml), sodium azide (211 mg, 3.25 mmol) was added slowly and the reaction mixture was stirred at 80 °C for 4 h. After it was cooled to room temperature, the reaction mixture was diluted with saturated aqueous $NaH_2PO_4$ and the mixture was extracted three times with AcOEt. The organic layer was washed twice with saturated $NaH_2PO_4$, once with brine, dried over anhydrous $MgSO_4$, filtered, and evaporated under reduced pressure. The residue was purified by silica gel column chromatography ($CHCl_3$/MeOH = 10/1 to 4/1), yielding **6-$N_3$DCF** (234 mg, 0.530 mmol, yield 50%) and **5-$NO_2$DCF (**155 mg, 0.348 mmol, yield 33%) as a red solid.

#### 2.3.3. 6-$N_3$DCF

$^1$H NMR (400 MHz, DMSO-$d_6$) δ 11.08 (2H, br), 7.98 (1H, d, $J$ = 8.2 Hz), 7.40 (1H, dd, $J$ = 8.2, 1.8 Hz), 7.13 (1H, d, $J$ = 1.8 Hz), 6.88 (2H, s), 6.71 (2H, s). $^{13}$C NMR (100 MHz, DMSO-$d_6$) δ 167.4, 155.1, 153.7, 150.0, 147.4, 128.3, 126.8, 122.2, 121.9, 116.2, 114.3, 110.2, 103.6, 81.0. HRMS (ESI-TOF) $m/z$ calculated: $C_{20}H_8N_3O_5Cl_2$ $[M - H]^-$: 439.9841, 441.9812, found: 439.9844 (+0.3 mmu), 441.9820 (+0.8 mmu).

#### 2.3.4. 5-$NO_2$DCF

$^1$H NMR (400 MHz, DMSO-$d_6$) δ 8.87 (1H, d, $J$ = 2.3 Hz), 8.38 (1H, dd, $J$ = 8.5, 2.5 Hz), 7.54 (1H, d, $J$ = 8.2 Hz), 6.67 (2H, s), 6.21 (2H, s). HRMS (ESI-TOF) $m/z$ calculated: $C_{20}H_{10}NO_7Cl_2$ $[M+H]^+$: 445.9834, 447.9805, found:445.9835 (+0.1 mmu), 447.9809 (+0.4 mmu).

#### 2.3.5. 6-Amino-2′,7′-dichlorofluorescein (6-$NH_2$DCF)

A solution of **6-$N_3$DCF** (150 mg, 0.340 mmol) and $Na_2S-9H_2O$ (163 mg, 0.677 mml) in $H_2O$ (3 ml) was stirred at 50 °C for 30 min. After the solution was cooled to room temperature, saturated aqueous $NaH_2PO_4$ was added to the mixture, and the mixture was extracted with AcOEt. The organic layer was then washed twice with saturated aqueous $NaH_2PO_4$, once with brine, then dried over anhydrous $MgSO_4$, filtered, and evaporated under reduced pressure. The residue was purified by silica gel column chromatography ($CHCl_3$/MeOH = 10/1 to 4/1) to give the title solid as an orange solid (101 mg, 0.242 mmol, yield 71%). $^1$H NMR (400 MHz, DMSO-$d_6$) δ 11.06 (2H, br), 7.60 (1H, d, $J$ = 8.2 Hz), 6.87 (2H, s), 6.78 (1H, dd, $J$ = 8.7, 1.8 Hz), 6.68 (2H, s), 6.37 (2H, s), 6.12 (1H, d, $J$ = 1.4 Hz). $^{13}$C NMR (100 MHz, DMSO-$d_6$) δ 168.4, 155.8, 155.3, 154.9, 149.8, 128.0, 126.4, 116.1, 115.9, 111.5, 111.4, 105.3, 103.6, 79.3. HRMS (ESI-TOF) $m/z$ calculated: $C_{20}H_{10}NO_5Cl_2$ $[M - H]^-$: 413.9936, 415.9907, found: 413.9940 (+0.4 mmu), 415.9915 (+0.8 mmu).

#### 2.3.6. 5-Amino-2′,7′-dichlorofluorescein (5-$NH_2$DCF)

A solution of **5-$NO_2$DCF** (101 mg, 0.227 mmol) and $Na_2S-9H_2O$ (206 mg, 0.857 mml) in $H_2O$ (2 ml) was stirred at 60 °C for 2 h. After the solution was cooled to room temperature, saturated aqueous $NaH_2PO_4$ was added to the mixture, and the mixture was extracted three times with AcOEt. The organic layer was then washed twice with saturated aqueous $NaH_2PO_4$, once with brine, then dried over anhydrous $MgSO_4$, filtered, and evaporated under reduced pressure. The residue was purified by silica gel column chromatography ($CHCl_3$/MeOH = 4/1) to give the title compound as an orange solid

Please cite this article as: M. Mori et al., Convenient synthesis of regioisomerically pure 5- and 6-functionalized xanthene dyes via $S_NAr$ reaction and comparison of their reactivity towards click reaction, Tetrahedron, https://doi.org/10.1016/j.tet.2020.131087

(40.1 mg, 0.0963 mmol, yield 42%). $^1$H NMR (400 MHz, DMSO-$d_6$) δ 11.08 (2H, br), 7.23–6.77 (5H, m), 6.65 (2H, s), 5.85 (2H, s). HRMS (ESI-TOF) *m/z* calculated: $C_{20}H_{10}NO_5Cl_2$ [M − H]$^-$: 413.9936, 415.9907, found: 413.9937 (+0.1 mmu), 415.9911 (+0.4 mmu).

*2.3.7. 5-Azido-2′,7′-dichlorofluorescein (5-$N_3$DCF)*

To a solution of **5-$NH_2$DCF** (24.1 mg, 0.0579 mmol) in AcOH/$H_2O$ (1.2 ml, 1:1), sodium nitrite (8.1 mg, 0.020 mmol) was added on ice and stirred on ice for 1 h. Sodium azide (11.7 mg, 0.180 mmol) was added to the reaction mixture and stirred on ice for 1 h. Then, the reaction mixture was stirred at room temperature for 1.5 h. After saturated $NaH_2PO_4$ was added to the mixture, the solution was extracted three times with AcOEt. The organic layer was washed twice with saturated aqueous $NaH_2PO_4$, once with brine, dried over anhydrous $Na_2SO_4$, filtered, and evaporated under reduced pressure. The residue was purified by silica gel column chromatography ($CHCl_3$/MeOH = 4/1) to give the title solid as an orange solid (20.5 mg, 0.0464 mmol, yield 80%). $^1$H NMR (400 MHz, DMSO-$d_6$) δ: 11.12 (2H, br), 7.63 (1H, d, $J$ = 1.8 Hz), 7.52 (1H, dd, $J$ = 8.2, 2.3 Hz), 7.36 (1H, d, $J$ = 8.2), 6.88 (2H, s), 6.73 (2H, s). HRMS (ESI-TOF) *m/z* calculated: $C_{20}H_8N_3O_5Cl_2$ [M − H]$^-$: 439.9841, 441.9812, found: 439.9845 (+0.4 mmu), 441.9819 (+0.7 mmu).

*2.3.8. 5(6)-Nitro-2′,7′-tetramethylrhodamine (5(6)-$NO_2$TMR)*

A suspension of 4-nitrophthalic anhydride (1.03 g, 5.33 mmol) and 3-(dimethylamino)phenol (1.65 g, 12.0 mmol) and polyphosphoric acid (105 mg) in DMF (30 ml) was stirred at 120 °C for 12 h. After cooling to room temperature, the solution was evaporated under reduced pressure. The residue was dissolved in methanol (5 ml) and the methanol solution was poured onto $H_2O$ (100 ml) on ice. The precipitate was collected by filtration and washed three times with ice-cold water. The residue was purified by silica gel column chromatography ($CHCl_3$/MeOH = 8/1 to 1/1) to give **5(6)-$NO_2$TMR** as a red solid (131 mg, 0.304 mmol, yield 6%).

*2.3.9. 6-Azido-tetramethylrhodamine (6-$N_3$TMR), 5-azido-tetramethylrhodamine (5-$N_3$TMR)*

To a suspension of **5(6)-$NO_2$TMR** (104 mg, 0.242 mmol/isomer, 5-isomer:6-isomer = 1:1) in NMP (2 ml), sodium azide (55.2 mg, 0.846 mmol) was added slowly and the reaction mixture was stirred at 80 °C for 3 h. After cooling to room temperature, the reaction mixture was diluted with saturated aqueous $NaHCO_3$. The precipitate was collected by filtration and washed three times with ice-cold water. The crude extract was purified by silica gel column chromatography twice ($CHCl_3$/MeOH = 10:1 and 1:1, respectively), yielding **6-$N_3$TMR** (13.9 mg, 0.0325 mmol, yield 13%) and **5-$NO_2$DCF** (44.1 mg, 0.102 mmol, yield 42%) as red solids.

*2.3.10. 6-$N_3$TMR*

$^1$H NMR (400 MHz, DMSO-$d_6$ plus 30% $DCl_{aq}$) δ 8.18 (1H, d, J = 8.7 Hz), 7.47 (1H, dd, J = 8.7, 2.3 Hz), 7.19 (1H, d, J = 2.3 Hz), 7.05 (2H, dd, J = 9.1, 2.3 Hz), 7.01 (2H, d, J = 9.6), 6.89 (2H, d, J = 2.3), 3.21 (12H, s). $^{13}$C NMR (100 MHz, DMSO-$d_6$ plus 30% $DCl_{aq}$) δ 165.7, 157.2, 157.1, 144.6, 135.8, 133.4, 131.0, 127.1, 121.1, 115.1, 113.3, 96.5, 40.9. HRMS (ESI-TOF) *m/z* calculated: $C_{24}H_{22}N_5O_3$ [M+H]$^+$: 428.1723, found: 428.1718 (−0.5 mmu).

*2.3.11. 5-$NO_2$TMR*

$^1$H NMR (400 MHz, DMSO-$d_6$) δ 8.64 (1H, d, $J$ = 1.8 Hz), 8.53 (1H, dd, $J$ = 8.5, 2.1 Hz), 7.49 (1H, d, $J$ = 8.7 Hz), 6.59 (2H, d, $J$ = 8.7 Hz), 6.51 (2H, d, $J$ = 2.3 Hz), 6.48 (2H, dd, $J$ = 8.7, 2.7 Hz), 2.94 (12H, s). HRMS (ESI-TOF) *m/z* calculated: $C_{24}H_{21}N_3O_5Na$ [M+Na]$^+$: 454.1379, found: 454.1371 (−0.8 mmu).

*2.3.12. 6-Amino-tetramethylrhodamine (6-$NH_2$TMR)*

A suspension of **6-$N_3$TMR** (34 mg, 0.078 mmol) and $Na_2S$–$9H_2O$ (88 mg, 0.37 mml) in MeOH/$H_2O$ (2 ml, 1:1) was stirred at 60 °C for 1 h. A suspension of $Na_2S$–$9H_2O$ (108 mg, 0.451 mml) in MeOH (1 ml) was added to the reaction mixture and stirred at 70 °C for 1 h. After the solution was cooled to room temperature, saturated aqueous $NaH_2PO_4$ was added to the mixture, and the mixture was extracted three times with AcOEt. The organic layer was washed with brine, then dried over anhydrous $MgSO_4$, filtered, and evaporated under reduced pressure. The residue was purified by silica gel column chromatography ($CHCl_3$/MeOH/MeCN = 4/1/1) to give the title solid as a brown solid (19 mg, 0.048 mmol, yield 62%). $^1$H NMR (400 MHz, DMSO-$d_6$) δ 7.55 (1H, d, $J$ = 8.2 Hz), 6.72 (1H, dd, $J$ = 8.5, 1.6 Hz), 6.65–6.36 (6H, m), 6.27–6.00 (3H, m), 2.93 (12H, s), $^{13}$C NMR (100 MHz, DMSO-$d_6$) δ 169.1, 155.4, 151.9, 151.8, 128.4, 125.8, 115.2, 112.6, 109.0, 107.4, 105.7, 97.9, 79.2, 39.9. HRMS (ESI-TOF) *m/z* calculated: $C_{24}H_{24}N_3O_3$ [M+H]$^+$: 402.1818, found: 402.1811 (−0.7 mmu).

*2.3.13. 5-Azide-tetramethylrhodamine (5-$N_3$TMR)*

A suspension of **5-$NO_2$TMR** (38.4 mg, 0.0891 mmol) and $Na_2S$–$9H_2O$ (101 mg, 0.422 mml) in $H_2O$/DMSO (2 ml, 1:1) was stirred at 60 °C for 30 min. After the solution was cooled to room temperature, saturated aqueous $NaH_2PO_4$ was added to the mixture, and the mixture was extracted three times with AcOEt. The organic layer was washed with brine, then dried over anhydrous $MgSO_4$, filtered, and evaporated under reduced pressure. The crude extract, obtained by column separation with silica gel ($CHCl_3$/$CH_3OH$ = 4/1 to 1/1), was used for the next reaction without further purification. To a solution of crude extract in $H_2O$/AcOH (1.2 ml, 1:2), sodium nitrite (18.9 mg, 0.274 mmol) was added and stirred on ice for 1 h. Then, sodium azide (21.0 mg, 0.323 mmol) was added and stirred on ice for 1 h and then at room temperature for 1.5 h. The solution was diluted with saturated $NaH_2PO_4$ and extracted three times with AcOEt. The organic layer was washed twice with saturated aqueous $NaH_2PO_4$, once with brine, dried over anhydrous $Na_2SO_4$, filtered, and evaporated under reduced pressure. The residue was purified by silica gel column chromatography ($CHCl_3$/MeOH = 4/1) to give the title compound as a dark purple solid (11.4 mg, 0.0267 mmol, yield 30% in two steps). $^1$H NMR (400 MHz, DMSO-$d_6$) δ 7.62 (1H, d, $J$ = 1.8 Hz), 7.48 (1H, dd, $J$ = 8.2, 2.3 Hz), 7.23 (1H, d, $J$ = 8.2 Hz), 6.55–6.44 (6H, m), 2.93 (12H, s). $^{13}$C NMR (100 MHz, DMSO-$d_6$) δ 168.0, 152.2, 152.0, 148.8, 141.5, 128.41, 128.37, 126.6, 125.6, 114.3, 109.0, 105.8, 98.0, 85.0, 39.8. HRMS (ESI-TOF) *m/z* calculated: $C_{24}H_{22}N_5O_3$ [M+H]$^+$: 428.1723, found: 428.1711 (−1.2 mmu).

## 3. Results

*3.1. Rationale and spectroscopic observation of DCF*

The synthetic utility of nitro groups as leaving groups for direct *ipso*-substitution with nucleophiles (e.g. azides, thiols, alkoxides) in dipolar aprotic solvents has been demonstrated in many types of reactions [21]. The structural requirement of *ipso*-substitution of the nitro group in nitroarenes is the presence of a functional group that stabilizes the transitional Meisenheimer complex at the *ortho*- or *para*-position.

A xanthene dye with a carboxylic group in the 3-position of the *meso*-phenyl ring forms a spirolactone ring via intramolecular nucleophilic attack of the carboxylate, which results in an equilibrium between the open (colored) and closed spirolactone (colorless) forms (Scheme 1). The position of equilibrium between the two xanthene isomers depends on the temperature, pH, hydrogen bonding ability, and self-organization of solvent, where protic

Please cite this article as: M. Mori et al., Convenient synthesis of regioisomerically pure 5- and 6-functionalized xanthene dyes via $S_NAr$ reaction and comparison of their reactivity towards click reaction, Tetrahedron, https://doi.org/10.1016/j.tet.2020.131087

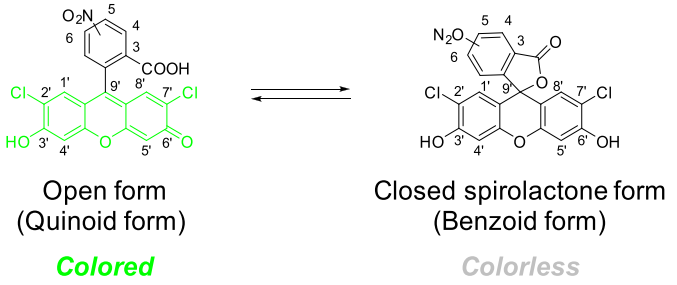


**Scheme 1.** Chemical equilibrium of 5(6)-nitro-2′,7′-dichlorofluorescein (DCF).

solvents favor the open form and aprotic solvents favor the closed spirolactone form [22,23]. In the closed spirolactone form, the nitro group of 5- or 6-$NO_2$DCF is in the *meta*- or *para*-position relative to the strong electron-withdrawing spirocyclic ester, respectively. Therefore, it is expected that the spirocyclic ester causes a difference in the reactivity of the *ipso*-carbon between the 5- and 6-$NO_2$DCF regioisomers and promotes the selective nucleophilic attack on the *ipso*-carbon of the 6-nitro group rather than the 5-nitro group (Scheme 2). To find a solvent that shifts the equilibrium to increase the proportion of the closed spirolactone form, the 5(6)-$NO_2$DCF regioisomeric mixture was dissolved in several aprotic dipolar solvents and the absorption spectra were measured (Fig. 1). While the 5(6)-$NO_2$DCF mixture shows high absorbance in $H_2O$ or *N, N*-dimethylformamide (DMF), it shows a dramatically lower absorbance in *N*-methylpyrolidone (NMP) and hexamethylphosphoric triamide (HMPA). Especially, the visible light absorption completely disappeared in HMPA. This result suggests that the equilibrium of 5(6)-$NO_2$DCF is shifted significantly to the closed spirolactone form in HMPA.

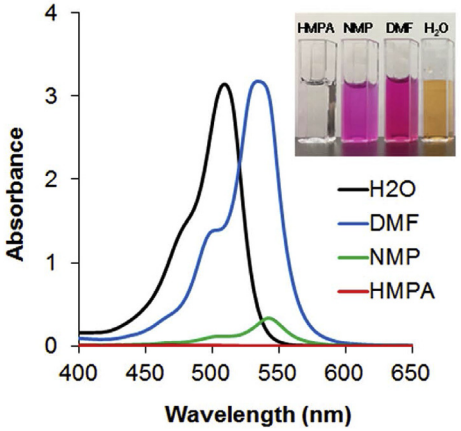


**Fig. 1.** Absorption spectra of 5(6)-nitro-DCF in various polar solvents. The inset shows the color of 5(6)-$NO_2$DCF (50 μM) in each solvent photographed under incandescent light.

### 3.2. Regioisomer selective $S_NAr$ reaction on 5(6)-$NO_2$DCF mixture

Next, we investigated the isomer-selective $S_NAr$ reaction of 5(6)-$NO_2$DCF in HMPA. For this purpose, sodium azide was used as a nucleophile, because azidated dyes are often used as synthetic intermediates and can be used for labeling experiments [11,12]. 5(6)-$NO_2$DCF was mixed with three equimolar of sodium azide and reacted in HMPA. Preliminary experiments showed no reaction at room temperature (data not shown), so the reaction was carried out at 80 °C. Reversed phase (RP)-HPLC analysis was performed to monitor the progression of the reaction. As the peak corresponding to 6-$NO_2$DCF gradually decreased, a new peak was observed to increase (Fig. 2A). After 2 h, the 6-$NO_2$DCF peak completely disappeared and the product peak reached its maximum. LC-MS analysis demonstrated that the product peak showed a molecular mass number corresponding to the expected reaction product, azide-substituted DCF. In contrast, no change in the 5-$NO_2$DCF peak was observed under these conditions (Fig. 2).

The same reaction was also carried out in NMP and DMF for comparison with HMPA. RP-HPLC analysis clearly revealed that the reaction proceeded in all the solvents tested, but the formation of the $S_NAr$ product differed greatly; with most formation in HMPA, less in NMP, and the least in DMF, which is the reverse order of the magnitude of the dipole moment (Fig. S1). Therefore, the results suggest that the formation of spirolactone promotes the $S_NAr$ reaction selectively toward 6-$NO_2$DCF.

After the regioselective $S_NAr$ reaction of 5(6)-$NO_2$DCF, 6-$N_3$DCF and 5-$NO_2$DCF were isolated from the reaction mixture through column chromatography. On the one hand, 6-$N_3$DCF was assigned by conventional spectroscopic measurements and $^1H-^{13}C$ HMBC NMR spectrum analysis (Fig. 3), then converted to 6-$NH_2$DCF (Scheme 3). On the other hand, 5-$NO_2$DCF was reduced to corresponding 5-$NH_2$DCF with sodium sulfide, and then followed by diazotization and subsequent treatment with sodium azide to yield

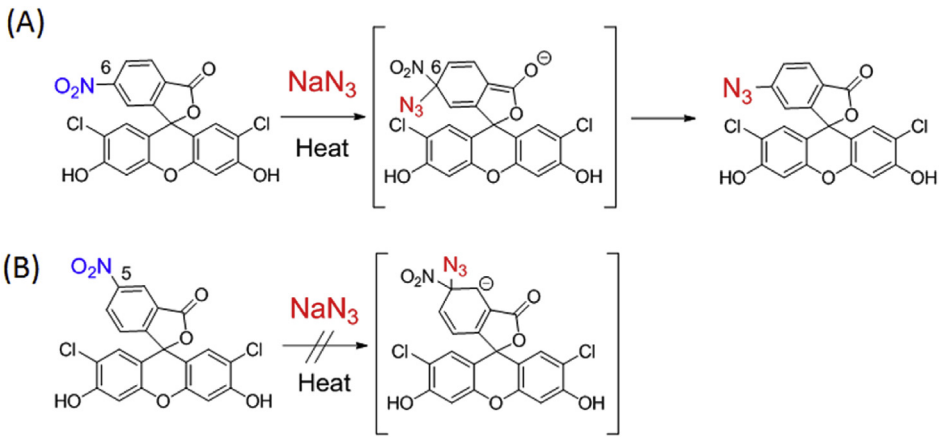


**Scheme 2.** Plausible mechanism of regioselective $S_NAr$ reaction of 6-$NO_2$DCF. (A) 6-$NO_2$DCF undergoes $S_NAr$ substitution by stabilizing the Meisenheimer complex with an electron-withdrawing spirocyclic ester in the *para* position. (B) 5- $NO_2$DCF does not react with sodium azide because there is no stabilizing factor for the Meisenheimer complex.

Please cite this article as: M. Mori et al., Convenient synthesis of regioisomerically pure 5- and 6-functionalized xanthene dyes via $S_NAr$ reaction and comparison of their reactivity towards click reaction, Tetrahedron, https://doi.org/10.1016/j.tet.2020.131087

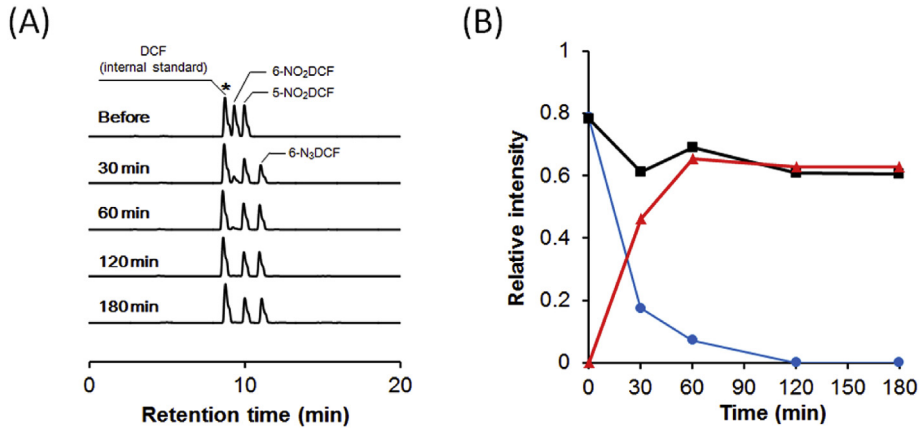


**Fig. 2.** (A) Time course of the RP-HPLC elution profile of the reaction mixture. Asterisk represents the peak of DCF as an internal control. At each time, an aliquot of the reaction mixture was mixed with DCF solution and subjected to RP-HPLC analysis. Absorbance at 505 nm was monitored for detection. (B) Time course of the content of each compound. Relative intensity represents corresponding peak relative to that of the DCF peak. 6-$N_3$DCF (Red triangles), 6-$NO_2$DCF (Blue circles), and 5-$NO_2$DCF (Black squares).

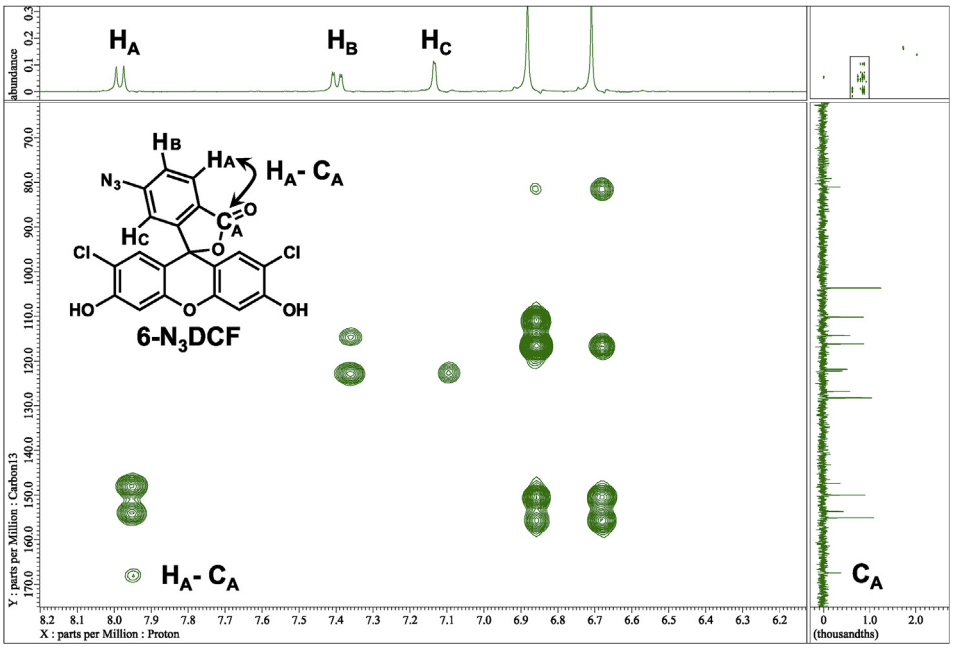


**Fig. 3.** $^{1}H–^{13}C$ HMBC NMR spectrum of 6-$N_3$DCF.

5-$N_3$DCF in 80% yield (Scheme 3). Taken together, this new synthetic strategy can be used to prepare each regioisomer of 5- and 6-functionalized DCF.

### 3.3. Regioisomer-selective $S_NAr$ reaction on the 5(6)-$NO_2$TMR mixture

Having successfully synthesized both the 5- and 6-regioisomers for each of $NH_2$- and $N_3$-DCF, we next asked whether this approach could be applied to rhodamine fluorophores. To examine this, tetramethylrhodamine (TMR) was chosen as the fluorophore because TMR is robustly used as the labeling reagent in studies of chemical biology [24,25] and biochemical applications [26,27]. 5(6)-$NO_2$TMR, prepared according to a previously reported procedure [17], completely lost visible light absorption in NMP and DMF among the aprotic dipolar solvents we tested (Fig. S2). This suggests that the equilibrium shifted from the open form to the closed spirolactone form in these solvents. Therefore, 5(6)-$NO_2$TMR was subjected to a reaction with sodium azide in NMP, resulting in the formation of 6-$N_3$TMR in 13% yield. 6-$N_3$TMR was reduced to 6-$NH_2$TMR in 62% yield, which can be a key intermediate for further synthesis. The remaining 5-$NO_2$TMR was also isolated and reduced to 5-$NH_2$TMR, followed by diazotization and subsequent treatment with sodium azide to provide 5-$N_3$TMR in 30% yield in two steps (Scheme S1). The isolated pure regioisomers were both assigned by conventional spectroscopic measurements. These results show that this regioselective $S_NAr$ reaction can be applied to different fluorophores and that both regioisomers of 5(6)-functionalized TMR can be easily synthesized individually.

### 3.4. Comparison of the reactivity of regioisomers on click reactions

It is important to acquire information on the changes in the spectroscopic properties and kinetics of the regioisomers during

Please cite this article as: M. Mori et al., Convenient synthesis of regioisomerically pure 5- and 6-functionalized xanthene dyes via $S_NAr$ reaction and comparison of their reactivity towards click reaction, Tetrahedron, https://doi.org/10.1016/j.tet.2020.131087

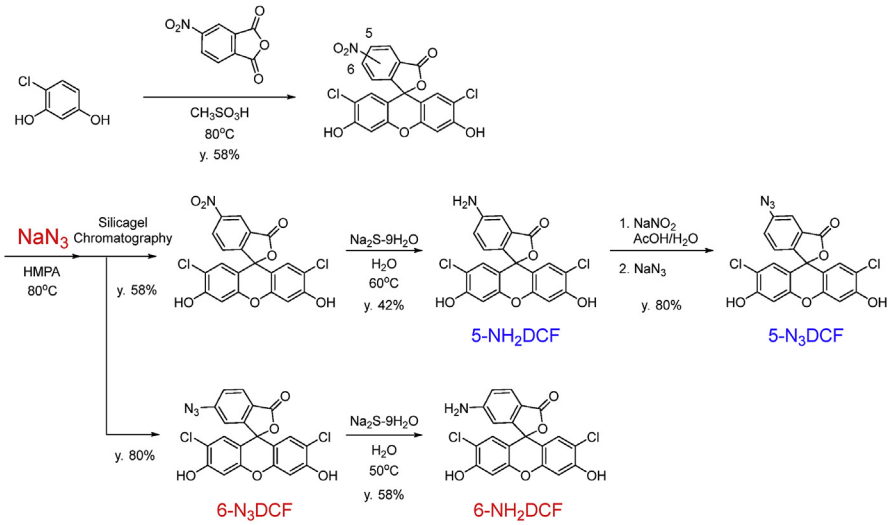


**Scheme 3.** The synthesis route for 5- and 6-substituted DCF.

click reactions. To this aim, we performed a comparative study of the regioisomers of $N_3$DCF in reactivity with an aliphatic cyclooctyne, BCN (Fig. 4A). BCN has unique properties among various cycloalkynes used for SPAAC and is more reactive with electron deficient azides [28]. We investigated whether the rate of the SPAAC reaction of BCN for the 5- or 6-isomer differs in different solvents. To examine the reactivity, each isomer of $N_3$DCF was incubated with BCN in phosphate buffered saline (PBS, pH 7.4) or several aprotic solvents for 30 min at room temperature. The reaction mixture was subjected to HPLC analysis to analyze the conversion of substrate to product. The data are summarized in Fig. 4B and C. When the SPAAC reaction was carried out in PBS, comparable product formation was observed between the two isomers. In contrast, in HMPA, the SPAAC reaction of $N_3$DCF yielded 1.5-fold more product derived from the 6-isomer than the 5-isomer (Fig. 4B). These results indicate that in HMPA, the 6-azide group is more reactive with BCN than the 5-azide group, consistent with the results obtained from the synthesis of 6-$N_3$DCF. Absorption and fluorescence spectra of each isomer of DCF were analyzed before and after the SPAAC reaction (Fig. 4C and D). During the click reaction, the change in maximum absorption or emission wavelength of 5-$N_3$DCF was only about 1 nm, whereas the 6-isomer showed a slightly larger bathochromic shift in both absorption and emission maxima, about 3 and 4 nm, respectively. In line with this observation, the quantum yield changed greatly from 0.727 to 0.744 for the 6-isomer, but only from 0.702 to 0.706 for the 5-isomer. These

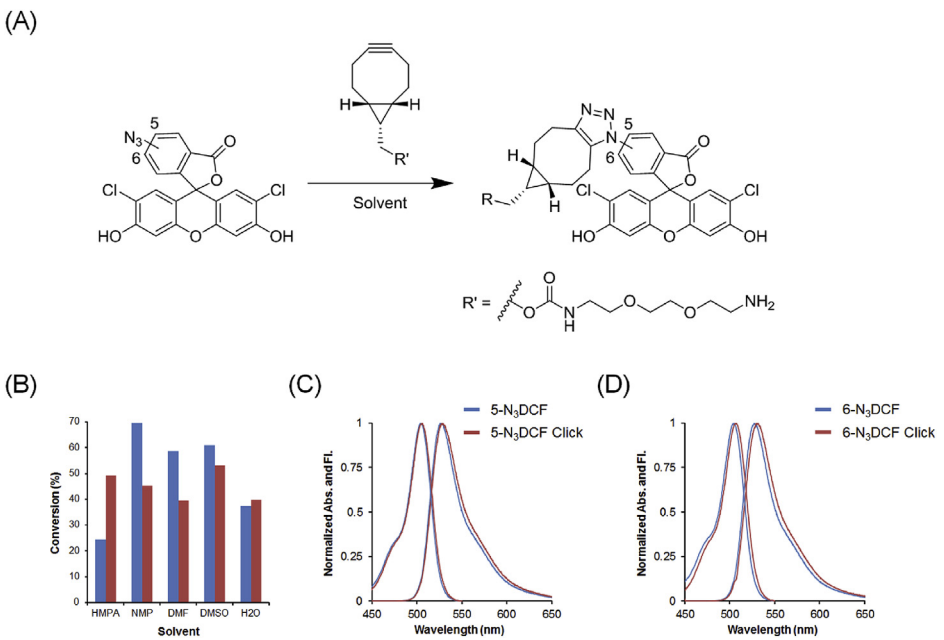


**Fig. 4.** Reactivity on SPAAC and change of spectroscopic properties of 5- or 6-$N_3$DCF. (A) Reaction of 5- and 6-$N_3$DCF with a BCN derivative. (B) Reactivity of 5- (blue column) and 6-$N_3$DCF (red column) with the BCN derivative in the SPAAC reaction. HPLC analysis of the reaction mixture gave peak areas corresponding to each compound (absorbance at 505 nm). The reaction was carried out in the indicated solvent containing either 5-$N_3$DCF or 6-$N_3$DCF and the BCN derivative for 1 h at 37 °C. Conversion was defined as the percentage of the formation of click product from the corresponding $N_3$DCF. (C, D) The normalized absorption and fluorescence spectra of 5-$N_3$DCF (C) and 6-$N_3$DCF (D). "$N_3$DCF Click" represents the reaction product of the SPAAC reaction.

Please cite this article as: M. Mori et al., Convenient synthesis of regioisomerically pure 5- and 6-functionalized xanthene dyes via $S_NAr$ reaction and comparison of their reactivity towards click reaction, Tetrahedron, https://doi.org/10.1016/j.tet.2020.131087

results suggest that the ground electronic state of the 6-$N_3$DCF is more susceptible to derivatization by the SPAAC reaction than that of the corresponding 5-isomer.

## 4. Conclusion

Here we report a simple procedure for the preparation of each isomer of 5(6)-functionalized DCF and TMR via regioselective $S_NAr$ reaction. In addition to those described here, this synthetic strategy is also applicable to other xanthene-based fluorophores such as rhodol and X-rhodamine, as long as optimal conditions such as solvents are determined. Therefore, this strategy is very versatile and simple for the preparation of labeling reagents or synthetic intermediates based on different regioisomers. Comparison of the labeling kinetics and the spectral and photophysical properties for each isomer highlighted the importance of preparing and comparing two different regioisomers. In conclusion, the synthetic strategy presented here helps expand the lineup of dyes that enable protein bioconjugation in chemical biology and biomaterials.

## Declaration of competing interest

The authors have no competing interests to declare.

## Acknowledgements

We appreciate Dr. Haruhiko Fukaya (Tokyo University of Pharmacy and Life Science) for help with HRMS measurements and Dr. Yasuteru Urano, Ryosuke Kojima (The University of Tokyo) for help with absolute quantum yield measurements. This research was supported by the Private University Research Branding Project of the Japanese Ministry of Education, Culture, Sports, Science and Technology; by MEXT/JSPS KAKENHI (18K05362) to Y.F.

## Appendix A. Supplementary data

Supplementary data to this article can be found online at https://doi.org/10.1016/j.tet.2020.131087.

## References

[1] R.P. Haugland, M.T.Z. Spence, I.D. Johnson, A. Basey, in: The Handbook: A Guide to Fluorescent Probes and Labeling Technologies, tenth ed., Molecular Probes, 2005. Molecular Probes.
[2] L.D. Lavis, Teaching old dyes new tricks: biological probes built from fluoresceins and rhodamines, Annu. Rev. Biochem. 86 (2017) annurev-biochem-061516-044839.
[3] G.Y. Mitronova, et al., Functionalization of the meso-phenyl ring of rhodamine dyes through SNAr with sulfur nucleophiles: synthesis, biophysical characterizations, and comprehensive NMR analysis, Eur. J. Org Chem. (2015) 337–349 (2015).
[4] G. Jiao, J.W. Han, K. Burgess, Syntheses of regioisomerically pure 5- or 6-halogenated fluoresceins, J. Org. Chem. 68 (2003) 8264–8267.
[5] A.H. Coons, J. Hugh, C.R. Norman, B. Ernst, The demonstration of pneumococcal antigen in tissues by the use of fluorescent antibody, J. Immunol. 45 (1942) 159–170.
[6] M.L. Smith, T.R. Carski, C.W. Griffin, Modification of fluorescent-antibody procedures employing crystalline tetramethylrhodamine isothiocyanate, J. Bacteriol. 83 (1962) 1358–1359.
[7] M. Abo, et al., Development of a highly sensitive fluorescence probe for hydrogen peroxide, J. Am. Chem. Soc. 133 (2011) 10629–10637.
[8] A. Wieczorek, P. Werther, J. Euchner, R. Wombacher, Green- to far-red-emitting fluorogenic tetrazine probes-synthetic access and no-wash protein imaging inside living cells, Chem. Sci. 8 (2017) 1506–1510.
[9] F.J. Huo, J. Kang, C. Yin, J. Chao, Y. Zhang, Highly selective fluorescent and colorimetric probe for live-cell monitoring of sulphide based on bioorthogonal reaction, Sci. Rep. 5 (2015) 2–6.
[10] A. Rotman, J. Heldman, Intracellular viscosity changes during activation of blood platelets: studies by fluorescence polarization, Biochemistry 20 (1981) 5995–5999.
[11] A. Salic, T.J. Mitchison, A chemical method for fast and sensitive detection of DNA synthesis in vivo, Proc. Natl. Acad. Sci. U. S. A 105 (2008) 2415–2420.
[12] C. Büll, et al., Steering siglec–sialic acid interactions on living cells using bioorthogonal chemistry, Angew. Chem. Int. Ed. 56 (2017) 3309–3313.
[13] K. Ajtai, et al., Stereospecific reaction of muscle fiber proteins with the 5' or 6' isomer of (iodoacetamido) tetramethylrhodamine, Biochemistry 31 (1992) 12431–12440.
[14] F. Stagge, G.Y. Mitronova, V.N. Belov, C.A. Wurm, S. Jakobs, Snap-, CLIP- and halo-tag labelling of budding yeast cells, PloS One 8 (2013) 1–9.
[15] T. Hirano, K. Kikuchi, Y. Urano, T. Higuchi, T. Nagano, Highly zinc-selective fluorescent sensor molecules suitable for biological applications, J. Am. Chem. Soc. 122 (2000) 12399–12400.
[16] Y. Fujikawa, Y. Urano, T. Komatsu, K. Hanaoka, H. Kojima, T. Terai, H. Inoue, T. Nagano, Design and synthesis of highly sensitive fluorogenic substrates for glutathione S-transferase and application for activity imaging in living cells, J. Am. Chem. Soc. 130 (2008) 14533–14543.
[17] H. Yu, Y. Xiao, H. Guo, From spirolactam mixtures to regioisomerically pure 5- and 6-rhodamines: a chemodosimeter-inspired strategy, Org. Lett. 14 (2012) 2014–2017.
[18] G.Y. Mitronova, et al., New fluorinated rhodamines for optical microscopy and nanoscopy, Chem. Eur J. 16 (2010) 4477–4488.
[19] S.J. Dwight, S. Levin, Scalable regioselective synthesis of rhodamine dyes, Org. Lett. 18 (2016) 5316–5319.
[20] J. Castro, A. Malakhov, K. Burgess, Synthesis of regioisomerically pure 5-functionalized 2′,7′-Dichlorofluoresceins, Synthesis (Stuttg) 7 (2009) 1224–1226.
[21] J.R. Beck, Nucleophilic displacement of aromatic nitro groups, Tetrahedron 34 (1978) 2057–2068.
[22] H. Leonhardt, L. Gordon, R. Livingston, Acid-base equilibriums of fluorescein and 2',7'-dichlorofluorescein in their ground and fluorescent states, J. Phys. Chem. 75 (1971) 245–249.
[23] D. Magde, G.E. Rojas, P.G. Seybold, Solvent dependence of the fluorescence lifetimes of xanthene dyes, Photochem. Photobiol. 70 (1999) 737–744.
[24] A.E. Speers, G.C. Adam, B.F. Cravatt, Activity-based protein profiling in vivo using a copper(I)-catalyzed azide-alkyne [3 + 2] cycloaddition, J. Am. Chem. Soc. 125 (2003) 4686–4687.
[25] R.N. Hannoush, N. Arenas-Ramirez, Imaging the lipidome: ω-alkynyl fatty acids for detection and cellular visualization of lipid-modified proteins, ACS Chem. Biol. 4 (2009) 581–587.
[26] K. Garai, C. Frieden, Quantitative analysis of the time course of Aβ oligomerization and subsequent growth steps using tetramethylrhodamine-labeled Aβ, Proc. Natl. Acad. Sci. U. S. A 110 (2013) 3321–3326.
[27] X. Li, T.M. Kapoor, Approach to profile proteins that recognize post-translationally modified histone 'tails', J. Am. Chem. Soc. 132 (2010) 2504–2505.
[28] J. Dommerholt, et al., Highly accelerated inverse electron-demand cycloaddition of electron-deficient azides with aliphatic cyclooctynes, Nat. Commun. 5 (2014) 1–7.

Please cite this article as: M. Mori et al., Convenient synthesis of regioisomerically pure 5- and 6-functionalized xanthene dyes via $S_NAr$ reaction and comparison of their reactivity towards click reaction, Tetrahedron, https://doi.org/10.1016/j.tet.2020.131087